

EOS Microwave Limb Sounder observations of upper stratospheric BrO: Implications for total bromine

Nathaniel J. Livesey¹, Laurie J. Kovalenko^{2,1}, Ross J. Salawitch¹, Ian A. MacKenzie³,
Martyn P. Chipperfield⁴, William G. Read¹, Robert F. Jarnot¹ and Joe W. Waters¹

Short title:

¹Jet Propulsion Laboratory, California Institute of Technology

²Columbus Technologies and Services Inc.

³University of Edinburgh

⁴Institute of Atmospheric Science, School of Earth and Environment, University of Leeds

1 **Abstract.** This paper describes new total stratospheric inorganic bromine (Br_y)
2 abundance estimates inferred from the first global observations of upper stratospheric BrO ,
3 made by the EOS Microwave Limb Sounder on the Aura satellite. Our ‘best estimate’ of
4 total upper stratospheric bromine loading (based on JPL-2002 kinetics with the addition
5 of a $\text{BrONO}_2 + \text{O}$ reaction) is 18.6 ± 5.5 pptv, for the period September 2004 to August
6 2005, from 55°S to 55°N . This implies a contribution of 3.0 ± 5.5 pptv from sources other
7 than long lived CH_3Br and halons. The possibility of such other sources has been raised
8 by balloon, aircraft and satellite observations of BrO in the lower and middle stratosphere.
9 These upper stratospheric observations provide new information to help resolve the current
10 uncertainty in stratospheric bromine loading. The abundance of bromine, particularly in
11 the lower stratosphere, is a significant factor in the budget of stratospheric O_3 .

12 Introduction

13 Stratospheric bromine and its role in photochemical O₃ destruction have received
14 much attention in recent studies [e.g., *Salawitch et al.*, 2005]. Estimates of total
15 stratospheric bromine loading based on observations of stratospheric BrO generally
16 indicate 4–6 pptv more bromine than would be expected from contributions of the known
17 long-lived source gases CH₃Br and halons [*WMO*, 2003]. This excess in total inorganic
18 bromine (Br_y) may reflect the contributions of short-lived halogenated species in the
19 stratosphere [e.g., *Wamsley et al.*, 1998; *Pfeilsticker et al.*, 2000] and of upper tropospheric
20 BrO transported into the stratosphere [*Pfeilsticker et al.*, 2000]. Either scenario implies
21 larger abundances of reactive bromine in the lower stratosphere than is often assumed in
22 model simulations of O₃ chemistry. In this region, where the bulk of the chlorine is still
23 in non-reactive organic forms, bromine plays a more significant role in photochemical O₃
24 destruction than elsewhere, and the rate of O₃ loss is very sensitive to the amount of Br_y
25 [*WMO*, 2003; *Salawitch et al.*, 2005].

26 In this paper new global observations of upper stratospheric BrO from the Microwave
27 Limb Sounder (MLS) [*Waters et al.*, 2006] on the Aura satellite (launched in July 2004)
28 are used in conjunction with models to infer upper stratospheric Br_y.

29 MLS BrO observations

Figure 1.

30 MLS observes two sets of BrO emission lines around 640 GHz. Figure 1 shows
31 observations from one of these sets. The 2–3 K noise on individual limb radiance
32 measurements is large compared to the typically 0.1–0.2 K signature of BrO. Significant
33 averaging is required to obtain abundance estimates with a useful signal-to-noise ratio.

34 Version 1.51 of the MLS data processing algorithms [Livesey *et al.*, 2006], the first
35 MLS data version released for public use, produces ~ 3500 BrO abundance profiles daily
36 with a typical precision of 200–300 pptv. When averages, such as monthly zonal means,
37 are taken, large amounts of noise are still seen in the data, due to a poor choice of the
38 tradeoff between precision and vertical resolution.

39 For this study, an ‘off-line’ BrO algorithm has been developed which produces a
40 pair of zonal mean abundance fields for each day, one for the ascending (mostly daytime)
41 part of the orbit, the other for descending (mostly nighttime). These are retrieved from
42 10° -latitude-resolution zonal averages of the daily radiance observations. Radiances are
43 binned onto a vertical grid of 12 surfaces per decade change in pressure (~ 1.5 km), using
44 the limb tangent point pressures from v1.51 data. The daily zonal mean BrO abundances
45 retrieved have an estimated precision of 10–20 pptv in the mid- and upper stratosphere.
46 Seasonal averaging of these gives abundances with a precision of ~ 2 pptv.

Figure 2.

47 Figure 2 shows seasonal zonal means of the ascending (a) and descending (b) MLS
48 BrO. These show the generally expected behavior, with ~ 9 –15 pptv of BrO seen in much
49 of the upper stratosphere during daytime and essentially zero BrO at night. Lower average
50 BrO abundances are seen on the ascending side of the orbit in polar night regions, while
51 significant abundance is seen on the descending half in the polar day regions.

52 The descending (mainly nighttime) BrO abundances observed by MLS are
53 unrealistically large around 10 hPa (larger still at greater pressures, not shown). For
54 pressures greater than about 4 hPa, essentially zero BrO is expected at night (2am
55 local time for MLS). The non-zero nighttime abundances therefore indicate systematic
56 biases. (See, however, Wahner *et al.* [1990] for observations of non-zero nighttime lower
57 stratospheric BrO, though those were for winter polar regions, not considered here). The

58 MLS biases, mainly due to inaccuracies in the retrieval method, become more significant
59 with increasing pressure, as line-broadening increases the contribution of other molecules
60 to the MLS radiances in the BrO spectral region.

61 Factors that give rise to these biases are expected to be constant between day and
62 night. Accordingly, the difference between day and night BrO observations is a more
63 accurate measure of daytime BrO. Figure 2c shows this difference for the MLS surfaces
64 between 10 and 4.6 hPa. In polar regions, the ascending and descending orbital phases
65 are often both day (summer) or night (winter), so differences in these regions are not
66 useful measures of daytime BrO and are not used in this study (see below for additional
67 discussion of the high-latitude summer data).

68 This study is confined to data between 55°S and 55°N, with ascending/descending
69 differences used as a measure of daytime BrO for pressures at and larger than the 4.6 hPa
70 MLS pressure surface, and ascending observations alone used for pressures at and
71 smaller than the 3.2 hPa MLS surface. For these latitudes, the local solar time of MLS
72 measurements ranges from 12:50pm to 2:30pm for the ascending part of the orbit, and
73 from 12:50am to 2:30am for descending.

74 **Accuracy assessment for the off-line BrO product**

75 Uncertainty in these observations divides into two categories. The first is precision
76 errors due to radiance noise, which can be reduced by averaging. The other category
77 is inaccuracies due to instrument calibration, spectroscopy uncertainty, and retrieval
78 approximations. These terms do not generally average down. However, in our case, neither
79 are they always manifested as temporally constant biases (as discussed below). Instrument
80 calibration and spectroscopic uncertainties are estimated to contribute, respectively, a

81 $\pm 20\%$ and $\pm 3\%$ uncertainty to the MLS BrO.

82 The accuracy of the retrieval algorithm is estimated by two independent techniques.
83 First, we take advantage of the fact that the off-line algorithms also retrieve O₃ and HNO₃
84 abundances that are based on observations of $\sim 1 - 2$ K emission lines of these molecules
85 in the vicinity of the BrO lines. One measure of the accuracy of the off-line algorithms is
86 therefore the level of agreement between these products and the well understood O₃ and
87 HNO₃ products produced by the version 1.51 algorithms, which use stronger lines from
88 these species. Second, the accuracy of the linearized forward model used in the retrievals
89 can be quantified by setting all the radiances to zero; the departure of the resulting BrO
90 from the expected zero abundance gives a measure of accuracy.

Figure 3.

91 Figure 3 shows the overall accuracy of the BrO product. This is the quadrature sum
92 of the $\pm 20\%$ calibration, the $\pm 3\%$ spectroscopic uncertainties, and the retrieval accuracy.
93 The latter is summarized as the worst accuracy at each level obtained from the three
94 independent estimates (O₃, HNO₃ and zero radiance). This gives an overall accuracy of
95 $\pm 30\%$ from 10–2.2 hPa. The 1.5 and 1 hPa data are excluded from further consideration
96 due to their poorer accuracy.

97 Again, note that these accuracy-related uncertainties are not expected to be constant
98 with time/latitude. For example, the accuracy of the retrieval algorithm is driven by
99 departure of the true atmospheric state (O₃, HNO₃, etc.) from that assumed in our
100 linearized forward model. Such errors will exhibit geographic and temporal variability.
101 Figure 2c shows a range of 11–16 pptv BrO for the mid-latitude ascending/descending
102 difference JJA 2005 BrO at ~ 6.8 hPa, a roughly $\pm 20\%$ scatter about the mean, well within
103 our estimated $\pm 30\%$ uncertainty.

104 Although we confine our studies to mid-latitudes, we note that Figure 2 shows

105 atypically large values of BrO ($\sim 18-20$ pptv) around 70°N over $10-4$ hPa during JJA
 106 2005 (70°S summer is similar). Day night differences – needed at these altitudes to reduce
 107 biases – cannot be taken for these polar day observations. However, studies of these biases
 108 show no reason why they should be larger for polar day. This is discussed further below.

109 Although there have been contemporaneous measurements of BrO obtained by
 110 balloon-borne instruments [*Pfeilsticker et al.*, 2000; *Pundt et al.*, 2002], few have had any
 111 overlap in altitude range. Future papers will compare these with MLS data.

112 **Using models to infer total bromine**

113 BrO is the dominant form of bromine in the daytime upper stratosphere, accounting
 114 for $\sim 60\%$ of the total bromine loading. Two models are used to infer the total stratospheric
 115 bromine abundance, needed to assess the impact of bromine on stratospheric O_3 .

116 **The SLIMCAT model**

117 For our analysis, the SLIMCAT model [*Chipperfield*, 1999] is run in ‘near-real time’
 118 driven by U.K. Met Office analysis fields. Model fields are sampled at the same locations
 119 and times (to the nearest 30 minute time step) as the MLS profile observations. By
 120 sampling the model in this manner, the diurnal cycle of BrO is fully taken into account.

121 Br_y is inferred according to

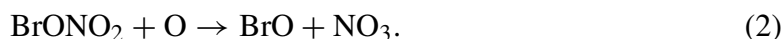
$$\text{Br}_y^{\text{MLS}} = \text{BrO}^{\text{MLS}} \left(\frac{\text{Br}_y^{\text{SLIMCAT}}}{\text{BrO}^{\text{SLIMCAT}}} \right). \quad (1)$$

122 This run of the SLIMCAT model has been initialized with 16 pptv CH_3Br and 6 pptv of
 123 Br_y (representing short lived sources) at the 326 K model boundary. The model shows
 124 all of the bromine in Br_y at pressures < 30 hPa. Details of the reactions and rates used in

125 both SLIMCAT and our other model are given below. The calculation in (1) is performed
126 for the daily zonal means of SLIMCAT BrO and Br_y, and MLS BrO (ascending and
127 ascending/descending difference, as described above). The resulting daily zonal mean Br_y
128 abundances are further averaged to increase the signal-to-noise ratio.

129 **The photochemical diurnal-steady-state box model**

130 In addition to SLIMCAT, a constrained diurnal photochemical steady-state model
131 [*Osterman et al.*, 1997] (PSS hereafter) is used to infer total bromine abundance from the
132 MLS BrO observations. This method was used similarly in *Sioris et al.* [2006]. The PSS
133 model is constrained to MLS observations of temperature, O₃ and water vapor, and also
134 to an NO_y abundance inferred from MLS N₂O observations using well established tracer
135 relations [*Popp et al.*, 2001; *Rinsland et al.*, 1996]. The total bromine loading is treated as
136 a free parameter that is iteratively adjusted until the modeled BrO abundance matches the
137 MLS observations. We ran the model with two sets of kinetics parameters. In one case,
138 which we call JPL02, we used JPL-2002 kinetics [*Sander et al.*, 2003]; in the other, which
139 we call JPL02a, we added the reaction [*Soller et al.*, 2001]



140 While not in the JPL-2002 compendium, this reaction has a large effect on stratospheric
141 bromine partitioning and is also included in SLIMCAT [*Sinnhuber et al.*, 2002].

142 As with the SLIMCAT calculation, the PSS model is run for the daily zonal mean
143 MLS BrO. The resulting daily Br_y zonal means are averaged to increase the signal-to-noise
144 ratio. As the daily zonal mean MLS BrO is noisy, negative values occur, which cannot be
145 handled by the PSS model. In these cases, the sign is reversed both on the BrO input to

146 PSS (to make it positive) and on the resulting Br_y (back to negative) before averaging.

147 **Comparison of Br_y inferred using two models**

Figure 4.

148 Figure 4 shows average Br_y profiles obtained using PSS (JPL02 and JPL02a cases)
 149 and SLIMCAT. These have been averaged over one year of MLS measurements, from
 150 55°S to 55°N . The models show good agreement at 10 hPa, but higher in the stratosphere
 151 SLIMCAT shows ~ 2 pptv more Br_y than PSS. This is mainly due to differences in the
 152 model abundances of O_3 and NO_y . SLIMCAT computes these, while PSS uses MLS O_3
 153 and NO_y inferred from MLS N_2O . When PSS is run using SLIMCAT O_3 and NO_y and
 154 constrained to SLIMCAT BrO , the inferred Br_y matches SLIMCAT's assumed 22 pptv Br_y
 155 abundance to within ± 0.6 pptv.

Figure 5.

156 Figure 5a compares the vertical profiles of O_3 used in the two models. In the 10
 157 to 2.2 hPa altitude range relevant to our calculation of Br_y , SLIMCAT O_3 is consistently
 158 lower than MLS observations (averages over shorter times show the same result). The
 159 lower O_3 abundance in SLIMCAT lowers the production rate of BrO via the reactions
 160 $\text{HOBr} + \text{O} \rightarrow \text{BrO} + \text{OH}$ and $\text{BrONO}_2 + \text{O} \rightarrow \text{BrO} + \text{NO}_3$, which in turn lowers the
 161 BrO/Br_y ratio, increasing the value of Br_y inferred from MLS BrO . In this altitude region,
 162 the MLS O_3 measurements have been shown to agree within 10% with other observations
 163 [Froidevaux *et al.*, 2006]. The O_3 deficit seen in the SLIMCAT model is well known [e.g.,
 164 Osterman *et al.*, 1997], although here it is occurring at altitudes lower than expected.

165 Similarly, there is a systematic difference between the NO_y abundances in the
 166 two models, with SLIMCAT consistently showing more NO_y than inferred from MLS
 167 measurements of N_2O . Although there are no independent measurements of NO_y , there
 168 are sunrise and sunset NO_2 data from the Halogen Occultation Experiment (HALOE)

169 [Gordley *et al.*, 1996] on board the Upper Atmosphere Research Satellite, which measured
170 NO₂ profiles by infrared solar occultation.

171 Figure 5b compares HALOE sunset data with sunset NO₂ produced by the PSS
172 model, using both tracer-relation-inferred NO_y from MLS N₂O and SLIMCAT NO_y.
173 (Since results at sunset are not output by our SLIMCAT run, we use the PSS model
174 to calculate the diurnal variation of the SLIMCAT model results). SLIMCAT clearly
175 overestimates the abundance of NO_y in this altitude range. The higher NO₂ in SLIMCAT
176 increases the loss rate of BrO via the reaction $\text{BrO} + \text{NO}_2 + \text{M} \rightarrow \text{BrONO}_2 + \text{M}$, again
177 increasing the value of Br_y inferred from MLS BrO.

178 **Results and discussions**

179 Further averaging of the results in Figure 4 (i.e., of Br_y averaged from 55°S to 55°N)
180 over the MLS pressure surfaces from 10 hPa to 2.2 hPa gives Br_y estimates of 20.7 pptv
181 from SLIMCAT and 19.2 and 18.6 pptv from PSS for the JPL02 and JPL02a cases,
182 respectively. All three values are estimated to be accurate to ±5.5 pptv. Of the three, the
183 JPL02a case (18.6 pptv) is considered the most accurate as it is based on the most realistic
184 atmospheric abundances of O₃ and NO_y and the most up-to-date reaction rates. The large
185 uncertainty in our results reflects the estimated ±30% accuracy of the MLS BrO product.
186 Future versions of the MLS data processing algorithms should improve this accuracy.

187 Taken at face value (i.e., without day/night differencing), the high latitude summer
188 BrO abundances discussed earlier imply a Br_y abundance of 24 pptv (PSS JPL02a) and
189 25 pptv (SLIMCAT). Both of these estimates are just outside the range of our result
190 from lower latitudes. Whether this indicates worse accuracy for these data (for which
191 day/night differencing was not possible) or poorly understood bromine partitioning will be

192 considered in future studies.

193 From MLS measurements of N₂O in this 10 hPa to 2.2 hPa, 55°S to 55°N region, and
194 the fact that we are considering a 1 year average, we estimate the year of stratospheric
195 entry [*Engel et al.*, 2002] of the air sampled in this study to be 2000±1. Tropospheric
196 CH₃Br and halons are estimated to have contributed 15.6 pptv total bromine at that
197 time [*Montzka et al.*, 2003]. This estimate, based on a global average of tropospheric
198 measurements of these gases obtained over the year 2000, accounts for a 7% loss of
199 CH₃Br in the troposphere, and thus provides a lower limit. A second estimate of 17.0 pptv
200 tropospheric CH₃Br and halons, based on projections from older data [*WMO*, 2003],
201 does not account for any tropospheric loss of CH₃Br, and thus provides an upper limit.
202 From the Montzka estimate, which is based on more recent data, our measurements imply
203 3.0±5.5 pptv of additional stratospheric bromine from other sources.

204 This compares well with the estimate of 3±3 pptv obtained from SCIAMACHY
205 observations [*Sinnhuber et al.*, 2005], though not so well with another estimate of
206 8.4±2 pptv, also from SCIAMACHY data [*Sioris et al.*, 2006]. Our observations are at the
207 lower range of the estimates given by *Pfeilsticker et al.* [2000] and *Salawitch et al.* [2005],
208 based on their analyses of aircraft and balloon data. Our results suggest a possible modest
209 contribution of 3.0±5.5 pptv from VSL bromocarbons to the stratospheric bromine budget.

Acknowledgments. The research described in this paper was carried out by the Jet
Propulsion Laboratory, California Institute of Technology, under a contract with the National
Aeronautics and Space Administration.

References

- Chipperfield, M. P. (1999), Multiannual simulations with a three-dimensional chemical transport model, *J. Geophys. Res.*, *104*, 1781–1805.
- Engel, A., M. Strunk, M. Muller, H. P. Haase, C. Poss, I. Levin, and U. Schmidt (2002), Temporal development of total chlorine in the high-latitude stratosphere based on reference distributions of mean age derived from CO₂ and SF₆, *J. Geophys. Res.*, *107*(D12), 4136.
- Froidevaux, L., et al. (2006), Early validation analyses of atmospheric profiles from EOS MLS on the Aura satellite, *IEEE Trans. Geosci. Remote Sens.*, *44*(5), 1106–1121.
- Gordley, L. L., et al. (1996), Validation of nitric oxide and nitrogen dioxide measurements made by the Halogen Occultation Experiment for the UARS platform, *J. Geophys. Res.*, *101*(10), 241–10,266).
- Livesey, N. J., W. V. Snyder, W. G. Read, and P. A. Wagner (2006), Retrieval algorithms for the EOS Microwave Limb Sounder (MLS), *IEEE Trans. Geosci. Remote Sens.*, *44*(5), 1144–1155.
- Montzka, S. A., J. H. Butler, B. D. Hall, D. J. Mondeel, and J. W. Elkins (2003), A decline in tropospheric organic bromine, *Geophys. Res. Lett.*, *30*(15), 1826, doi:10.1029/2003GL017745.
- Osterman, G. B., R. J. Salawitch, B. Sen, G. C. Toon, R. A. Stachnik, H. M. Pickett, J. J. Margitan, J. F. Blavier, and D. B. Peterson (1997), Balloon-borne measurements of stratospheric radicals and their precursors: Implications for the production and loss of ozone, *Geophys. Res. Lett.*, *29*(9), 1107–1110.

- Pfeilsticker, K., W. T. Sturges, H. Bösch, C. Camy-Peyret, M. P. Chipperfield, A. Engel, R. F. M. Müller, S. Payan, and B. M. Sinnhuber (2000), Lower stratospheric organic and inorganic bromine budget for the Arctic winter 1998/99, *Geophys. Res. Lett.*, 27(20), 3305–3308.
- Popp, P. J., et al. (2001), Severe and extensive denitrification in the 1999–2000 Arctic winter stratosphere, *Geophys. Res. Lett.*, 28(15), 2875–2878, doi:10.1029/2001GL013132.
- Pundt, I., J. P. Pommereau, M. P. Chipperfield, M. V. Roozendael, and F. Goutail (2002), Climatology of the stratospheric BrO vertical distribution by balloon-borne UV–visible spectrometry, *J. Geophys. Res.*, 107(D4), 4806, doi:10.1029/2002JD002230.
- Rinsland, C. P., et al. (1996), ATMOS measurements of H₂O+2CH₄ and total reactive nitrogen in the November 1994 Antarctic stratosphere: Dehydration and denitrification in the vortex, *Geophys. Res. Lett.*, 23(17), 2397, doi:10.1029/96GL00048.
- Salawitch, R. J., D. K. Weisenstein, L. J. Kovalenko, C. E. Sioris, P. O. Wennberg, K. Chance, M. K. W. Ko, and C. A. McLinden (2005), Sensitivity of ozone to bromine in the lower stratosphere, *Geophys. Res. Lett.*, 32, L05,811, 10.1029/2004GL021504.
- Sander, S. P., et al. (2003), Chemical kinetics and photochemical data for use in atmospheric studies, evaluation number 14, *Tech. rep.*, Jet Propulsion Laboratory, Pasadena, CA.
- Sinnhuber, B. M., et al. (2002), Comparison of measurements and model calculations

- of stratospheric bromine monoxide, *J. Geophys. Res.*, *107*(D19), 4398, doi:10.1029/2001JD000940.
- Sinnhuber, B. M., et al. (2005), Global observations of stratospheric bromine monoxide from SCIAMACHY, *Geophys. Res. Lett.*, *23*, L20,810, doi:10.1029/2005GL023839.
- Sioris, C. E., et al. (2006), Latitudinal and vertical distribution of bromine monoxide in the lower stratosphere from SCIAMACHY limb scattering measurements, *J. Geophys. Res.*, in press.
- Soller, R., J. M. Nicovich, and P. H. Wine (2001), Temperature-dependent rate coefficients for the reactions of $\text{Br}(^2\text{P}_{3/2})$, $\text{Cl}(^2\text{P}_{3/2})$ and $\text{O}(^3\text{P}_J)$ with BrONO_2 , *J. Phys. Chem. A*, *105*, 1416–1422.
- Wahner, A., J. Callies, H. P. Dorn, U. Platt, and C. Schiller (1990), Near uv atmospheric absorption-measurements of column abundances during Airborne Arctic Stratospheric Expedition, January–February 1989 3: BrO observations, *Geophys. Res. Lett.*, *17*(4), 517–520.
- Wamsley, P. R., et al. (1998), Distribution of halon-1211 in the upper troposphere and lower stratosphere and the 1994 total bromine budget, *J. Geophys. Res.*, *103*(D1), 1513–1526.
- Waters, J. W., et al. (2006), The Earth Observing System Microwave Limb Sounder (EOS MLS) on the Aura satellite, *IEEE Trans. Geosci. Remote Sens.*, *44*(5), 1075–1092.
- WMO (2003), World meteorological organization, scientific assessment of ozone depletion, *Tech. rep.*, World Meteorological Organization, Geneva Switzerland.

Figure Captions

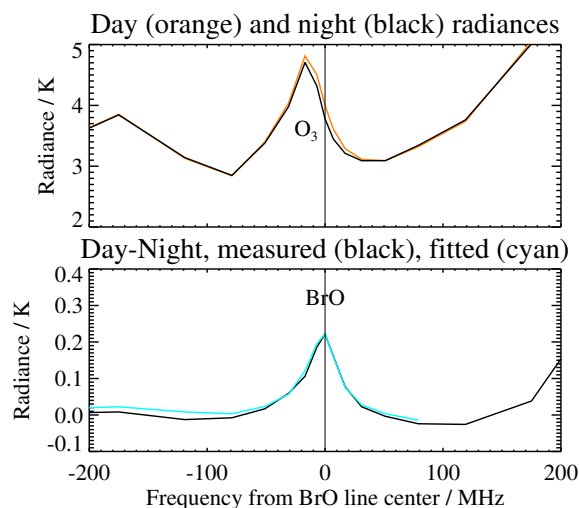


Figure 1. Top: average upper stratospheric MLS radiances observed in the region of the 650.19 GHz BrO lines. Black line is radiances measured during the descending (nighttime) part of the Aura orbit, orange is ascending (daytime). Average is from 55°S to 55°N, for limb rays with tangent pressures between ~ 10 hPa and 3.3 hPa, for the period September 2004 to August 2005. The emission signature of an isotopic O_3 line is indicated. Bottom: difference between day and night measured radiances (black). The BrO spectral signature is clearly seen, due to the strongly diurnal nature of BrO at these altitudes. Cyan line shows the fit achieved to this signal by the retrieval algorithm described in the text.

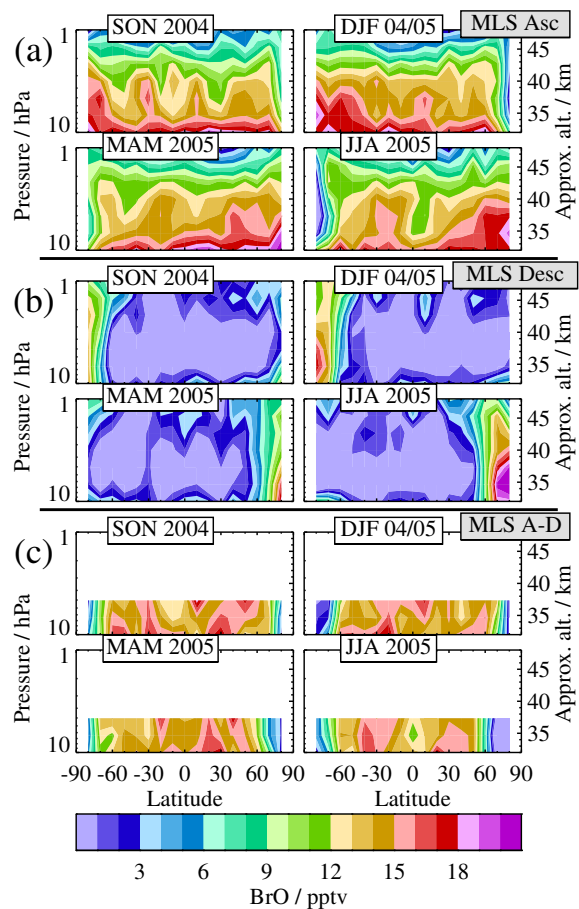


Figure 2. Seasonal zonal means of MLS BrO observations from (a) the ascending (mainly daytime) and (b) descending (mainly nighttime) phases of the orbits. The precision on these averages is 1–2 pptv over the vertical range shown. To alleviate biases in the lower regions, the difference (c) between ascending and descending can be used as a measure of daytime BrO at low and mid-latitudes, so long as the expected nighttime abundance of BrO is negligible, which is the case for MLS data on the 4.6 hPa and greater pressure surfaces.

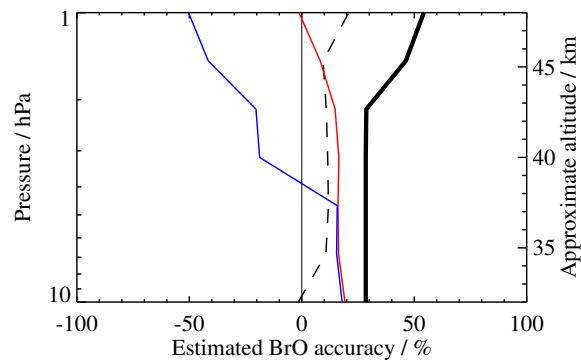


Figure 3. The estimated accuracy of the off-line BrO product. The red and blue lines show the estimates inferred from study of the offline O₃ and HNO₃ products, respectively. The dashed line shows the accuracy predicted from retrievals of zero radiance (scaled from pptv using the annual average 55°S to 55°N profile). The heavy black line shows the overall accuracy estimate, computed as the largest value of the three other lines which is then quadrature summed with the $\pm 3\%$ spectroscopy and $\pm 20\%$ calibration contributions. This results in an estimate of $\pm 30\%$ over the 10–2.2 hPa range.

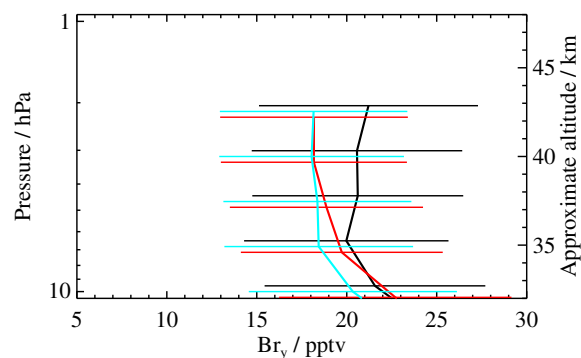


Figure 4. Average Br_y inferred from MLS data using the SLIMCAT (black) and PSS models (red with JPL02 kinetics, cyan with JPL02a). Average is from September 2004 through August 2005, over latitudes from 55°S to 55°N. Error bars reflect the $\pm 30\%$ accuracy of the MLS BrO.

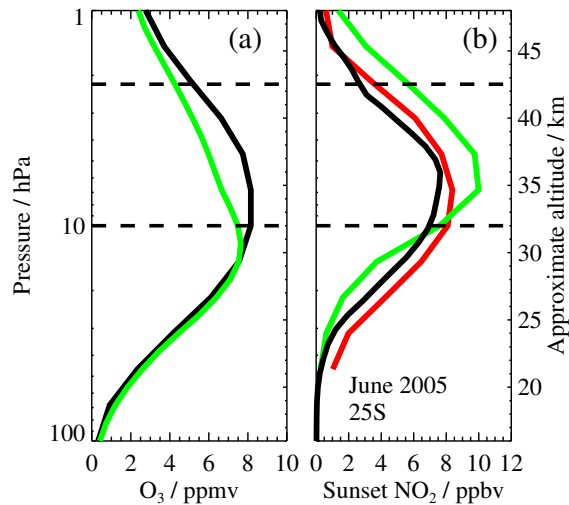


Figure 5. Comparison of vertical profiles of (a) O_3 and (b) NO_2 for the SLIMCAT (green) and PSS (red) models. The dashed lines bracket the relevant altitude region. In (a) the PSS model is constrained to MLS O_3 (black). The profiles are the September 2004 to August 2005 average from 55°S to 55°N . In (b) sunset NO_2 for both models is compared with HALOE data (black). Model daily zonal mean sunset NO_2 are averaged over June 2005 from 15°S to 35°S . The HALOE data (version 19) are averaged over June 2005 from 20°S to 30°S .